DYNAMIC AND QUASI-STATIC TENSILE PROPERTIES OF STRUCTURAL S400 STEEL

G. H. Majzoobi

Bu-Ali-Sina University, Hamadan, Iran

G. H. Farrahi

Sharif University of Technology, Tehran, Iran

(Received: June 3, 1999 - Accepted in Revised Form: September 30, 1999)

Abstract The study of mechanical behavior of the structural steel S400 under quasi- static and dynamic loading has been the subject of this investigation. In oder to obtain different stress - triaxiality conditions the specimens were notched with 1, 1.5, 2 and 3.5 mm notch radius. The results of fractography show as the velocity of tension increases, ductility reduces and a ductile-brittle transition occurs under certain stress triaxiality or strain rates. The observation of load-time history diagrams and SEM micrographs show that, as far as the fracture is ductile, any increase in velocity leads to the reduction of fracture load which is presumed to be due to reduction of plastic deformation. In brittle fracture, however, the velocity increase results in increase in fracture load which is thought to be due to micro-cracks formed at different level near to the fracture surface of specimens, the so called crack shielding and crack branching at high deformation velocities. Notch radius also proved to be highly effective on fracture mechanism which is due to notch strengthening. The change in grain size of some of the specimens shows that the ductile to brittle transition in fracture mechanism can be postponed by a suitable heat-treatment scheme up to a certain strain rate.

Key Words Dynamic, Behavior, Strain Rate, Fracture Mechanism, S400-Steel

ÙĎÚÉ@ÏÙh Î ÙĎÚś@Ru? Ø@Ó1@K m\? Qbš S400 Ê@ÈRg@u hÝÏµ ÙĎÚÍ@ĎÉ l@RµI ÕĊ\@¤É Ñ¼@¸É ËÙ? ªÏ ¡ ÏÉ æiéª_ ª@Ċy @K l?h ² @Ďy ª ÏÍ n? w Ù@ÉnA hlÏÉ Ø@ÓÑÍÏÈÍ *Øi ĊK Ñu wÌŠ n? PÎ@´RÉ £ãmy ÊhlÎA Quh ÑK Ø?mK -iy@KÙÉ Qċmåu wÙ?oå µ? @åK Ñâ½ iÌÓhÙÉ Ê@xÍ Ùµ?mÁÏR¼mµ YÙ@RÍ -iÍiÚhmÁ H@fRÍ? mRÈÚÁÚÉ 1,3 Î 0 */,3 */ Ø@Ó ² @Ďy mÚÚ°Š hmŠ ÑK ÆmÍ Q¼@c n? ËÚĊÉ Ø@Ó ² @Ďy ª@Ċy Î wÍm½ Ø@ÓdmÍ lh Q tĎy ÆoÚÍ@ĎÉ Î ÑR¼@Û wÓ@½ ÙÉmÍ *wx½ Q tĎy lh Ñ½ *QµmÁ ÑZÚRÍ Ê?ÏšÙÉ ÙÍÎmRĎ!? L ÏĎuÎmĎÚÉ mÛÎ@ | Š Î Ê@Én åÎmÚÍ Ø@Ól?hÏÈÍ Õ¨cÞÉ n? -i K@ÛÙÉ Ñâ\ ÙÁÎ? Ñâ½ *hhmÁÙÉ Q tĎy ØÎmÚÍ wÙ?o µ? I [ÏÉ *hmŠ Q tĎy lh Î ÎmÚÍ wÓ@½ I [ÏÉ Qċmu wÙ?o µ? *ÆmÍ oÚÍ Î hl?h Æ@Í ÙRfu º mŠ FcÞ¤ã? Ñ½ ÑÍÏÈÍ lh º mŠoÛl h@Z\? n? Ùy@Í ÙÉÎh Î č ÚRuÞ0 ÃĎy mÚÚ°Š wÓ@½ Q¼ċ Î Ðh@åÉ l@Rå µl må\ ·ÚÈå¿ mÚ\DŠ oÚÍ ² @Ďy ª@Ċy *ËÚÏ^ÈÓ -iy@KÙÉ ÃĎy mÚÚ°Š h@Ûn Qċmu m\? m\ @Ó º mŠ H@ĊxÍ? @ÓÑÍÏÈÍ n? Øh? iĊS Øi Ì\ ÑÍ?h l@Rg@u mÚÚ°Š -iy@KÙÉ ÙRfu ² @Ďy Æ@Í ÑK ØmRÉ?l@0 n? Ùy@Í Ñ½ hl?h Q tĎy ÆoÚÍ@ĎÉ wÍm½ dmÍ n? ÙÌÚĊÉ ic @Š ?l Q tĎy ÆoÚÍ@ĎÉ mÚÚ°Š ÙŠl?mc P@ÚÁÈ¿ I u@ÌÉ ÕÉ@Ím\ č Ù @K Ê?ÏšÙÉ Ñ½ h?h Ê@xÍ oÚÍ -Qg? iÍ? mÚgDŠ Ñ\

INTRODUCTION

Numerous applications of structural materials involve dynamic or impact types of loading. In order to design or analyze dynamically loaded structures more accurately, it is necessary to know mechanical behavior and properties of the materials involved at the strain rates to which the structure components are subjected. This paper is a progress report on a large-scope investigation into failure initiation of S400 steel under quasi-static and dynamic tests.

It is well known that the mechanical behavior of most materials are influenced to some extent by strain rate [1,2]. The magnitude

of such strain rate effects, especially in metals, has been a topic of numerous research projects since 1950¨s. Progress in this area, however, has been hampered by the lack of a reliable test technique for determining the mechanical behavior of metals at high strain rates. One of the major breakthroughs in this area was the development of Hopkinson bar [3]. Other devices such as cam-plastometer and Lindholm machine [4] have also been used by some researchers over past several decades. All high rate testing machines (tensile, compressive, and torsional) have some advantages and some disadvantages. It is not within the scope of this paper to review the aspects of these machines. However, a brief discussion of the high rate tensile testing machine called,"Flying Wedge", [5] which has been designed and constructed by the authors and been used in the present work seems necessary.

Our investigation had three main objectives:

(a) to subject the material to different stress states and to record the load - time histories to evaluate the effect of strain rate on rupture load.

(b) to study the fracture surfaces on the microscopic scales to obtain information on fracture mechanism using the scanning electron microscopy , SEM, [6].

(c) to obtain knowledge about the notch effect on fracture behavior. The first difficulty which faces an investigation into the effect of stress state (notch) on fracture is the choice of a suitable test specimen. Possible specimens have been discussed by McClintock [7]. In this investigation round tension specimens with pre-machined circumferential notches were chosen as being most suited for present requirements. Failure initiates in the central region of the notches of different severity. Also, the state of stress and strain rate can then be estimated by Bridgman theory [8]. This is concerned with the study of variation of stress triaxiality parameter versus fracture strain which is an important subject in ductile fracture simulations. Of course, this part of investigation is not reported here and will be given in subsequent papers.

TEST APPARATUS

The apparatus described here is a modified version of the ¨Flying Wedge¨ tensile testing machine [9]. A general view of the apparatus is

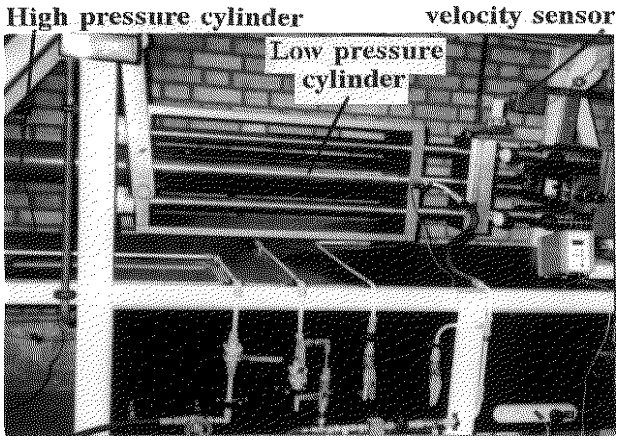

Figure 1. A general view of Flying wedge.

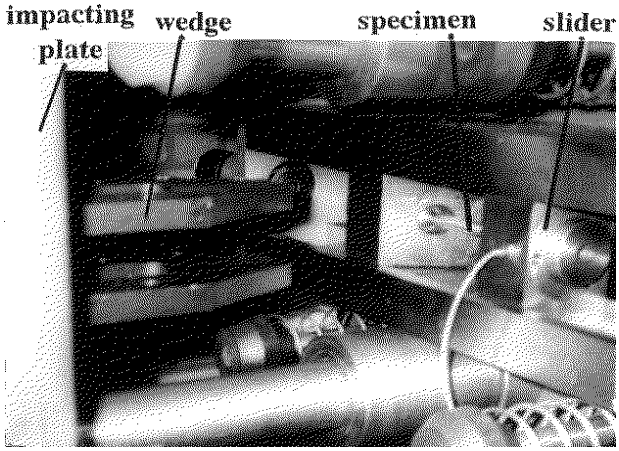

Figure 2. A closed-up picture of slider mechanism of Flying wedge.

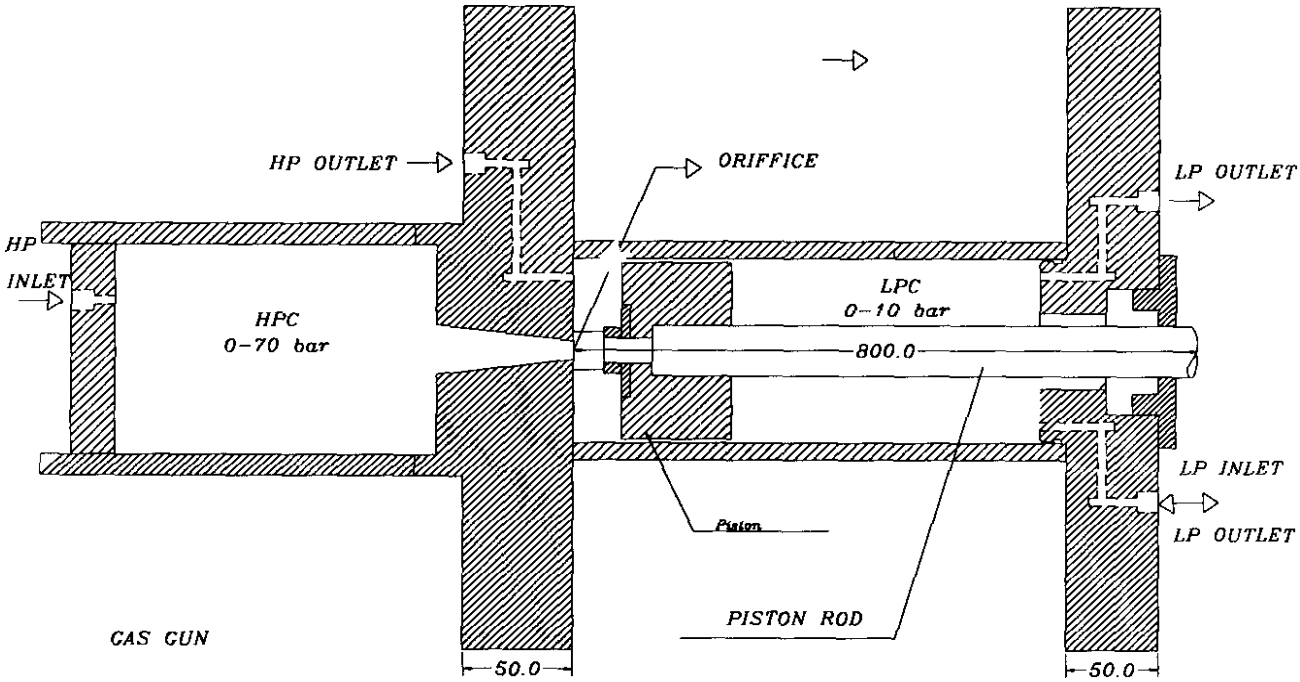

Figure 3. Gas-gun configuration of Flying wedge.

shown in Figures 1 and 2. This machine consists of three main parts: (a) propulsion system or gas gun, (b) slider mechanism , and (c) instrumentation system.

The gas gun, shown in Figure 3, consists of two high and low pressure cylinders (HPC and LPC) which are linked through an orifice, a wedge plate on which the impacting wedge is mounted and a piston which can freely slide in the low pressure cylinder and which is attached to the wedge by a piston rod. The HPC allows storage of high pressure compressed air which is then released quickly to the low pressure cylinder to accelerate the wedge. The low pressure air (up to 10 bar) inside LPC and behind the piston and high pressure air (up to 70 bar) in HPC are adjusted in such a way that the piston is held against the orifice by balancing the forces resulting from low and high pressures acting on the piston in opposite directions.

To fire the rig, the low pressure air is released and as a result, the additional force on the piston moves it from its equilibrium position and unseals the orifice. The high pressure air then acts on the full piston area and produces the force required to accelerate the wedge.

Slider mechanism, shown in Figure 2, consists of two sliders the angle of which match up with the wedge angle. The sliders track has been adjusted in such a way that the sliders can only move at right angles to the motion of the wedge. Specimens are fitted between two specimen holdrs which are placed into the sliders.

When the gas gun is fired, the impacting plate connected to the piston rod moves quickly and hits the sliders. As a consequence of the impact, sliders move away from each other resulting in tension of the specimen.

The deformation velocity can be varied in 3 different ways: (a) changing the wedge angle, (b) the air pressure in HPC, and (c) the notch radius. In the present work only 28 semi -

wedge angle has been used.

The test rig has been equipped with pressure, wedge and slider velocity , and load-time history measuring systems. The pressure of the two cylinders are monitored by pressure transducers of the type V440/P440 made by Digitron Instrumentation. The transducers are able to measure the pressure up to 100 bar within 0.01 bar accuracy. The load-time history is measured by a 120 KN piezoelectric load-cell made by Kistler ltd. This load-cell which has a hollow disk type shape , is placed into one of the sliders in such a way that it is subjected to a compressive load exactly equal to the tensile load of the specimen when it is pulled by sliders movement. The output voltage from load - cell which is very small is first rectified by a 5011 Kistler type amplifier and then is transferred to a computer via an SOB-8300 osilloscope board. The load-time history can be either displayed on a monitor or stored for further processing. Velocity of wedge (impact velocity) and slider (tension velocity) are measured by two velocity sensors consistsing of a high radiance emitter and a receiver called slotted switches. After firing , a narrow opaque strip mounted on the impacting plate or slider passes through the slot of the switch. The light emitted to the receiver can not be transmitted through the strip. The light transmition from emitter to receiver is monitored by the slotted switches via the SOB-8300 board onto a computer. The time to the passage of strip through the slotted switches is measured and the velocity is obtained by V= b/t in which b is the width of the strip.

MATERIALS AND SPECIMENS

The geometry of specimens are shown in Figure 4. In addition to plain specimens, notched specimens with 1, 1.5, 2 , and 3.5 mm notch

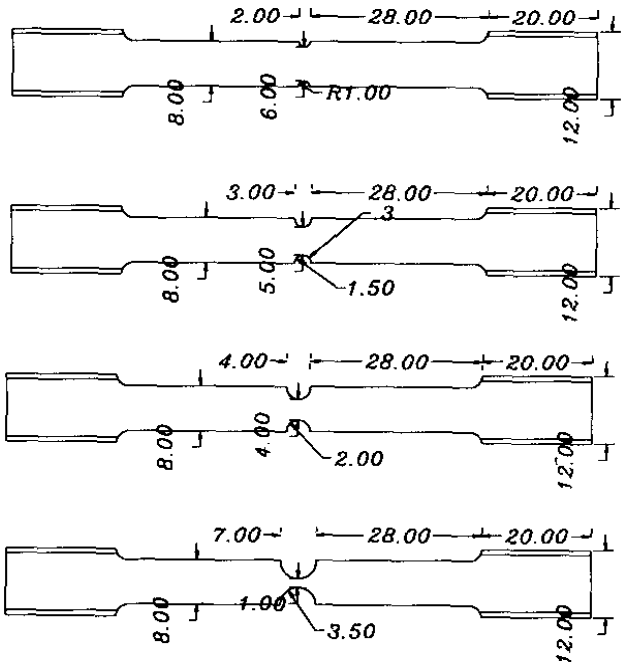

Figure 4. Geometry of the specimens with different notch radius.

radius were used in the investigation. The specimens were prepared from the reinforced bar structural steel S400, made by Iran¨s Steel Complex, which is widely used in constructions and in particular in reinforced concrete. The chemical analysis of the material shows that the material contains, 0.62% Si, 0.22%S, 1.53% Mn and 0.22% C, and the remainder of Fe. Also , the yield stress and the ultimate strength of the material, obtained from tensile test, found to be430 MPa and 650 MPa, respectively. In addition to as received specimens , two series of specimens with 1.5 mm notch radius were heat-treated to obtain a new grain structure. This was acheived by using two different heat treatment scheme. At first, all specimens were annealed at 900ùC and quenched in oil. Then, half of the specimens were tempered at 200ùC and were cooled in furnace , and the other half were tempered at 600ùC and were cooled in furnace. The specimens used for experiments are classified in Table 1.

TABLE 1. The Specimens Used for Experiments.

Serie	A	B	C	D	E	F	G
heat-treatment condition	as received	as received	as received	as received	as received	tempered at 600C	tempered at 200C
notch radius (mm)	à	3.5	2	1.5	1	1.5	1.5
gauge length (mm)	60	7	4	3	2	3	3

TEST PROGRAM

The main objective of this investigation was to load the specimens up to fracture to examine the micro-and macro-structural features of the deformed specimens after fracture. This was carried out through the following steps :

(a) All series of specimens were tested quasi-statically and dynamically at the impact velocities of 2.5 , 3.5 , an 6.5 m/ s. Quasi - static tests were performed on an Instron machine at rate of 10^{-3} S^{-1} , and the dynamic tests were carried out on the "Flying wedge" at strain rates up to 10^{3} S^{-1}. At each test, load-time history and velocity of impact were recorded for further processing.

(b) The fracture radius, r, (radius of the fracture section) and the profile radius , R , of the notch were measured. The fracture strain, e_f, was measured from $e_f = 2 \ln \frac{r}{r_o}$ (r_o= initial notch radius). There were two ways of evaluating strain rate in the deforming material: (i) $e = \frac{e_f}{t_f}$, in which t_f is the time to fracture obtained from load-time history, and (ii) $e = \frac{V_s}{L_o}$ in which V_s is the slider velocity and L_o is the initial gauge length of the specimen. Slider velocity was obtained from $V_s = V_w \tan 28$ in which V_w is the impact velocity [5].

(c) metallographic and fractogrophic examination of the fractured specimens were performed using optical and scanning electron microscopy.

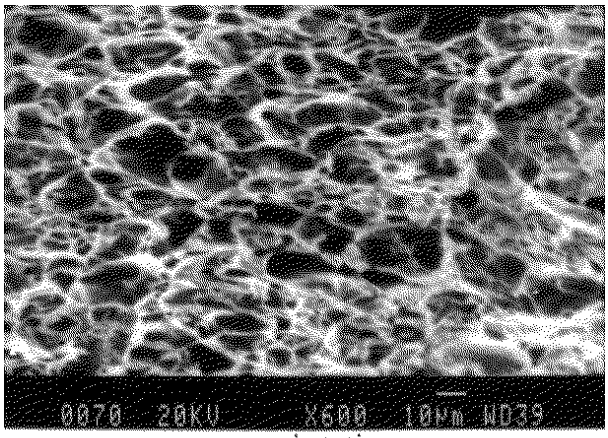

quasi-static

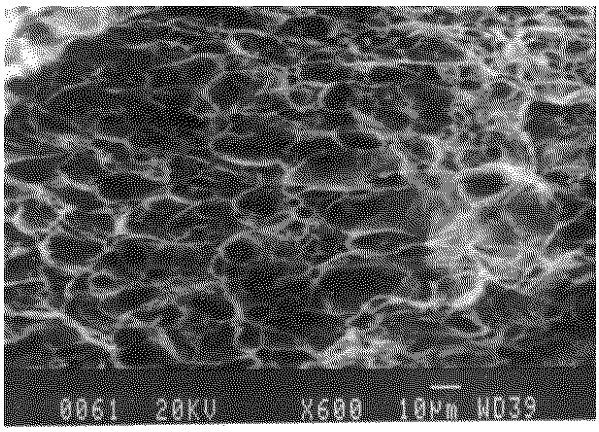

V = 6.5 m/s

Figure 5. Fracture surfaces of specimens with 3.5 mm notch radius.

(d) from the load-time history and velocity records the variation of fracture force versus strain rate for different series of specimens and the fracture force- notch radius curves for different impact velocities were plotted on separate graphs.

RESULTS AND DISCUSSION

The fracture surface of notched specimens tested at different velocities are illustrated in Figures 5 to 12. The variation of fracture load

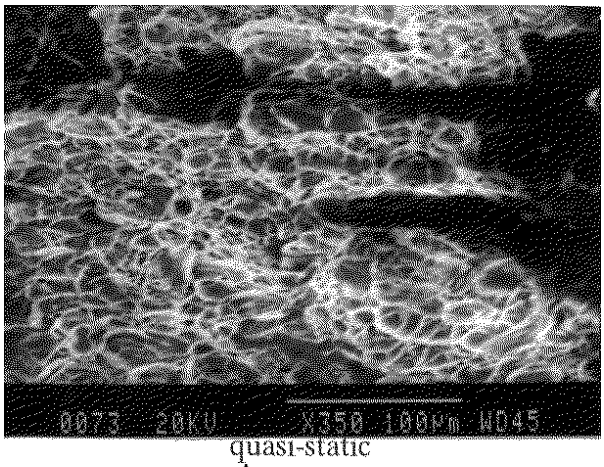

quasi-static

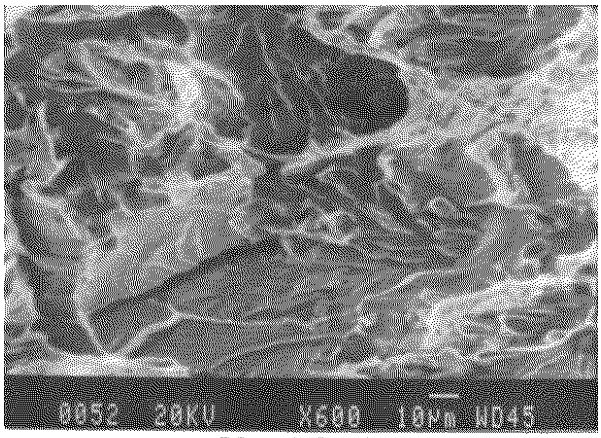

V = 3.5 m/s

Figure 6. Fracture surfaces of specimens with 2 mm notch radius.

versus velocity (F-V diagram) and fracture load versus notch radius (F-R diagram) are shown in Figures 13 and 14, respectively.

A quick study of these figures reveals that the mechanical behavior of the material is evidently influenced by notch radius or stress triaxiality, impact velocity or strain rate, and heat treatment condition. Therefore, it may be more useful to study the effect of each of these parameters separately.

(i) Tension Velocity Effects The F-V diagram for as received specimens (series B to E) is shown in Figure 13. With regard to the fact that the study of the manner of variation of fracture

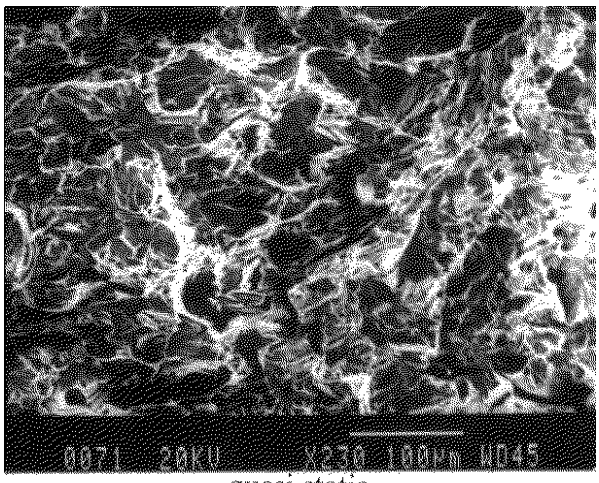

quasi-static

Figure 7. Fracture surface of specimen with 1.5 mm notch radius.

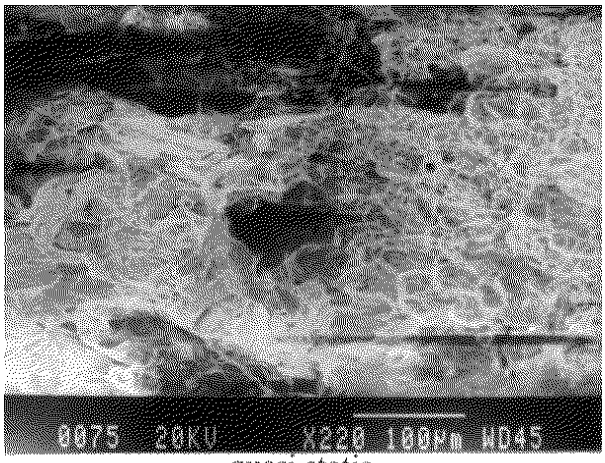

quasi-static

Figure 8. Fracture surface of specimen with 1 mm notch radius.

load (F) versus impact velocity and notch radius constitutes the main objective of this investigation rather than the evaluation of the magnitude of fracture load itself, the value of F is given in millivolts as obtained from the load cell output. As it can be seen, each curve on the diagram descends to a minimum point and thereafter begins to rise. The observation of the SEM micrographs shown in Figures 5 to 10 also reveals that the fracture mechanism is quite brittle at velocities higher than the value

corresponding to the minimum fracture load. The fracture mechanism, however, is either ductile or brittle before the minimum point.

The softening effect of the velocity in the descending part of the diagram can be explained by the fact that for ductile fracture (as for 2 and 3.5 mm notch radii) , plastic deformation is due to the mobility of dislocations which is affected by deformation velocity. As a result, at high tension velocity dislocations have less chance to move leading to reduction in the amount of plastic deformation. This subject is verified by SEM micrographs corresponding to fracture surfaces of specimens with 3.5mm notch radius tested quasi-statically and at 6.5 m/s, (Figure 5). As it can be seen, the number of dimples has reduced with increasing velocity. The softening effect of deformation velocity for specimens with 1 and 1.5 mm notch radius which exhibit brittle behavior even at low deformation velocities, can be explained in a manner similar to that of ductile specimens. In this case, the number of cleaves on the fracture surface reduces with velocity up to a certain value. The hardening effect of strain rate or impact velocity on the ascending part of F-V diagram may be explained by two phenomena : (a) crack branching; When a brittle fracture occurs at a high velocity, any crack which attains to its maximum growth rate begins to branch and as a result, new cracks develop at high

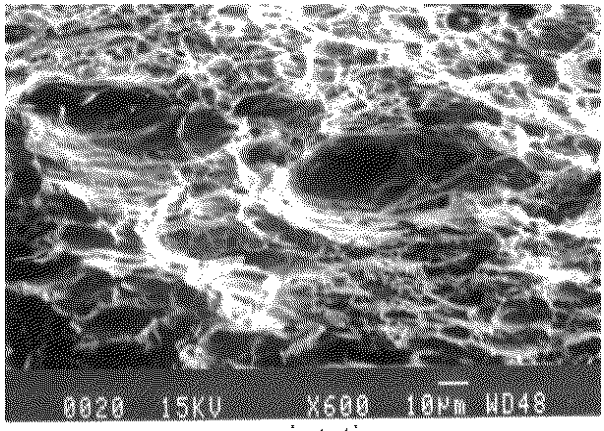

quasi-static

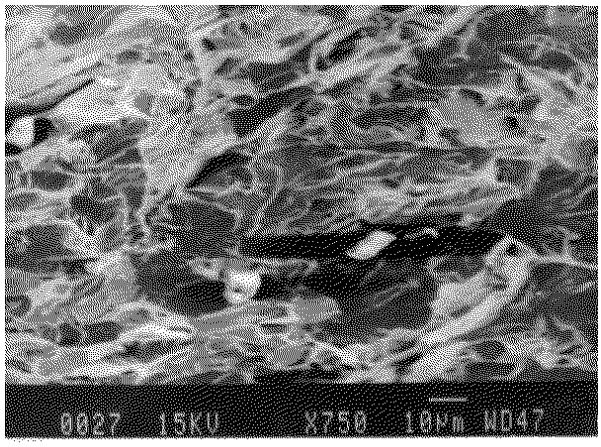

V = 3.5 m/s

Figure 9. Fracture surfaces of specimens tempered at 200 °C.

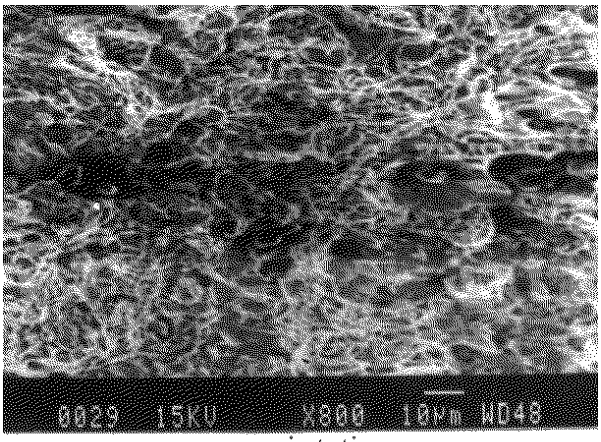

quasi-static

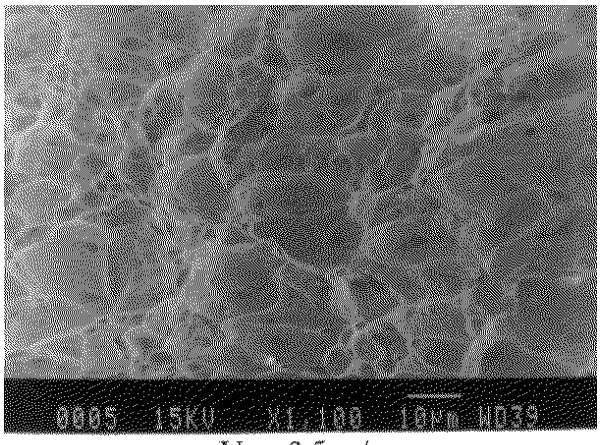

V = 3.5 m/s

Figure 10. Fracture surfaces of specimens tempered at 600 °C.

impact velocities (see Figure 11), The growth of new cracks require additional force giving rise to the increase in fracture load. (b) Crack shielding; which is often used to increase the strength of ceramics. This phenomenon happens when micro - cracks known as secondary cracks develop at different levels close to the fracture surface of specimen. These cracks turn into barriers against the growth of the main crack which is responsible for fracture of the specimen. In other word, when the main crack meets the secondary cracks, it is deviated to a new route. These deviations reduce the crack growth rate and lead to strengthening of the material.

(ii) Notch Radius Effects In order to study the effect of notch radius, we begin to examine the fracture surface of specimens with different notch radius under quasi- static loading . As it can be seen in Figures 5 to 8, the fracture surface of tested specimens changes from a quite dimpled surface (ductile fracture) for 3.5 mm notch radius to a cleaved surface (brittle fracture) for 1.5 and 1 mm notch radius. The reason for this change of fracture mechanism is stress triaxiality at notch region which become more severe as the notch radius reduces. Stress triaxiality is expressed by parameter P/Y in which Y is yield stress of the material and P is hydrostatic pressure ($P = \sigma_i/3$) . This parameter is approximately defined by the following relation [8]:

$$P/Y = \frac{1}{3} + \mathrm{Ln}\left(\frac{r}{2R} + 1\right) \quad (1)$$

in which r is the radius of fracture section and R is the profile radius of the notch after fracture. It has been found by many researchers that fracture strain ($e_f = 2 \ln \frac{r_o}{r}$) is inversely proportional to exponential of P/Y. One of the early equations in this field proposed by Hancock and Mackenzie [10] is the following:

$$e_f = \left(D_1 + D_2 \exp\left(-\frac{3}{2} P/Y\right)\right) \quad (2)$$

in which D_1 and D_2 are constants ($D_1 = 0.2$ for steel) . The relations between P/Y and e_f are used for numerical simulations of ductile fracture. The results of this part of investigation will be given in details in the next paper. However , we may arrive at the conclusion that P/Y which increases with fracture strain reduction, leads to a brittle transition in fracture mechanism as the notch radius or e_f, reduces. Table 2 gives the fracture strains measured for tested specimens with various notch radius.

The SEM micrographs shown in Figures 6 (Q.S.) and 12 which correspond to the fracture surfaces of 2 mm and 3.5 mm notched specimens, respectively, indicate that the

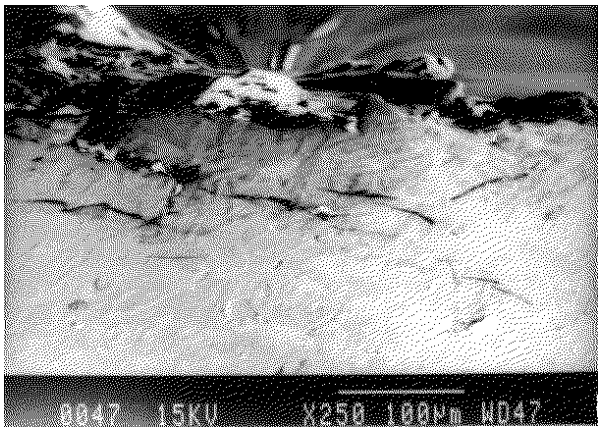

Figure 11. Secondary cracks produced at high impact velocity.

TABLE 2. Fracture strains measured for various notch radius.

notch radius (mm)	3.5	2	1.5	1
e_f	80%	40%	32%	18%

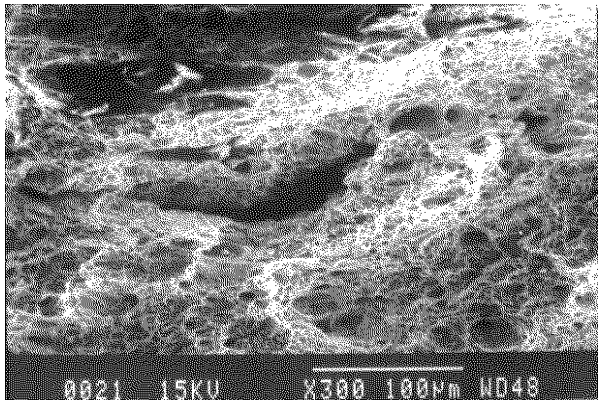

Figure 12. Fracture surface of a specimen with 3.5 mm notch radius.

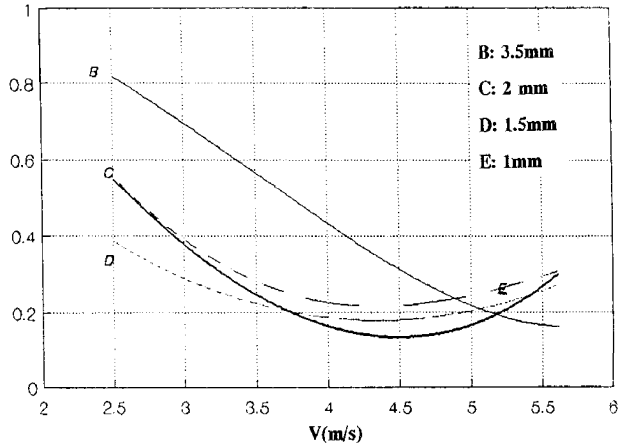

Figure 13. Fracture load-impact velocity diagrams for as-received specimens.

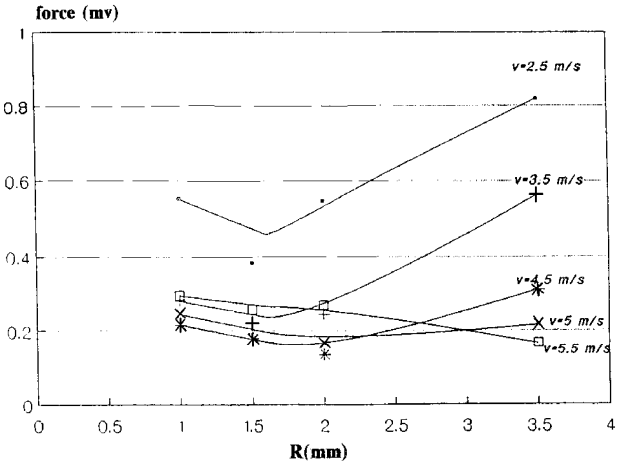

Figure 14. Fracture load-notch radius diagram for different impact velocities.

number of dimples considerabely has reduced for 2 mm specimen. This agrees with anapproach of ductile fracture which is based on statistical measurements of a large number of microscopic voids, which are nucleated and grow to observable size in ductile fracture. Inthis approach which has been extensively used by many researchers such as Barbee et al [11], the number, size and orientation of voids or microcracks in brittle fracture are determined. Then from the experimental data, the nucleation and growth rate of voids are obtained and a damage criterion which correlates these parameters to material properties is derived.

A useful diagram of fracture load versusnotch radius of various tension velocity is shownin Figures 13 and 14. The change in the trend of curves shown in this figure can be attributed to the effects of two parameters: notch strengthening and crack shielding.

Notch strengthening is due to the plastic region developed in the vicinity of the notch appex. These plastic stresses are overcome by reactive stresses exerted by the elastic portion of the specimen surrounding the plastic region. So, an additional force is required to overcome the plastic stresses. As the notch radius decreases, the plastic region is more expanded and the specimen is more strengthened. The crack shielding phenomenon was described in the first part of this section. Now the F-R curves shown in Figure 14 and the corresponding SEM micrographs shown in Figures 5 to 10 can be explained as follows:

In the first part of the diagram in which the F-R curves are descending, the notch strengthening and crack shielding have the same effect, because as the notch radius decreases, the number of cracks produced in the specimen and the effect of notch strengthening increase.

However, in the second part of the curves the fracture mechanism is ductile and the effect of notch also diminishes. As a result, after a certain notch radius , say 1.5 or 2mm , the effect of notch decreases with velocity increase.

(iii) Heat-Treatment Effects - The fracture surface of the specimens (with 1.5 mm notch radius) tempered at 200ùC (serie G) and 600ùC (serie E) are shown in Figures 9 and 10, respectively. While, the behavior of as received specimens with 1.5 mm notch radius were quite brittle in quasi-static conditions (see Figure 7), the Figures 9 and 10 represent a ductile behavior for heat-treated specimens, indicating that heat-treatment has softening effect to some extent on the material. These effects, however, are more profound for the specimens tempered at 600ùC than those tempered at 200ùC.

The F-V curves for the heat-treated specimens (series E and G), not shown here, had the same trend as for the E-V curves already explained for as received specimens, namely, the curves descend to an extremum point and thereafter begin to rise.

This is consistent with SEM micrographs of fracture surfaces in Figures 9 and 10 which show a ductile fracture (dimpled surface) up to a certain velocity indicated on the figures. Higher velocities than those shown on the figures result in a brittle fracture and their corresponding SEM micrographs are not shown here. In general, it can be concluded that a convenient heat treatment scheme may be used to soften the material and postpone the change of fracture mechanism to a certain deformation velocity, to avoid an undesired and unpredicted failure of a structure which may happens due to a change in mechanical behavior or fracture mechanism.

REFERENCES

1. Meyers M. A., "Dynamic Behavior of Materials", John Wiley & Sons, Printed in U. S. A., (1994).
2. Blazynski T. Z. "Materials at high strain rates", Elsvier Applied Science, Printed in Hong Kong., (1987).
3. Nicholas T., "Dynamic Tensile Testing of Structural Materials using a Split Hopkinson Bar Apparatus", AF WAL-TR-80-4053, Wright Patterson AFB, (Aug. 1980).
4. Lindholm U. S., "High Strain Rate Tests, Techniques of Metal Research", Vol. V, pp 199-253, (1971).
5. Majzoobi G. H., "Design and Manufacturing of High Strain Rate Testing Machine", Research Report, 32-892, Bu - Ali Sina University, (1998).
6. Van Stone R. H. and Cox T. B., "Use of Fractography and Sectioning Techniques to Study Fracture Mechanics", ASTM STP 600, American Society of Testing Materials, pp 5-29, (1976).
7. McClintock F. A., "Plasticity Aspects of Fracture; An Advanced Treatise", (Ed Liebowitz), Vol. III, p 47. Academic press, New York ,(1971).
8. Bridgman P. W., "Studies in Large Flow and Fracture", McGraw Hill, New York, (1952).
9. Majzoobi G. H., "Experimetal and Numerical Studies of Metal Deformation and Fracture at High Strain Rates", Ph. D. Thesis, Leeds University, (1990).
10. Hancock J. W. and Mackenzic A. C., "On the mechanism of ductile failure in high strength subjected to multiaxial stress-states", ***J. of Mechanical Physics and Solids***, Vol. 24, pp 147-169, (1976).
11. Barbee T. W., Seaman L., Crewdson R. and Curran D., "Dynamic fracture criteria for ductile and brittle metals", ***J. of Materials***, Vol. 7, pp 393-401, (1972).